



EXPERIMENTAL ASSESSMENT OF CIRCULAR COLLAR EFFECT ON LOCAL SCOUR AROUND SINGLE CYLINDRICAL PIER AND NUMERICAL INVESTIGATION OF FLOW STRUCTURE

Ahmed M. Helmi¹, Ahmed H. Shehata², Muhannad M. Abbas³ and
Mohamed S. El-manadely⁴

¹Assistant Professor, ²Assistant Professor and ³Ph.D. Candidate, ⁴Professor of Hydraulics, Irrigation and Hydraulics department, Faculty of Engineering, Cairo University, Giza, Egypt.

المخلص

ظاهرة النحر المحلي حول دعامات الجسور من المشاكل الواسعة الانتشار و استخدمت طرق عديدة لتقليل عمق النحر و منها استخدام الياقات التي تفاوتت تققيم اثرها بين الباحثين، و تهدف الدراسة الي فحص تأثير الياقات على النحر المحلي وعلى طبيعة التدفق حول دعامة مفردة اسطوانية الشكل، حيث تم اجراء تجارب معملية بأستخدام اقطار ومناسيب مختلفة للياقة المثبتة حول الدعامة الاسطوانية المفردة للحصول على افضل قطر وافضل منسوب للياقة لتقليل عمق النحر المحلي حول الدعامة وايضا الحصول على الشكل النهائي لحفرة النحر بعد الوصول الى زمن الاستقرار، و تم عمل نمذجة عددية ثلاثية الابعاد باستخدام (ANSYS FLUENT) لتمثيل التجارب المعملية، و تم الوصول الي اقل عمق نحر باستخدام ياقة بقطر يساوي اربعة اضعاف قطر الدعامة علي منسوب يساوي نصف قطر الدعامة اسفل منسوب القاع قبل النحر. و اتضح من النمذجة العددية تاثير الياقة علي تقليل مركبة السرعة الراسية بمقدار 20% و كذلك مساحة نفوذها مما ادي الي تخفيض عمق النحر بمقدار 53%

ABSTRACT

Scouring around bridge piers is a dominant parameter in pier foundation design, and dramatically affects the construction cost. Collars are one of the local scour countermeasures, based on the concept of flow alternation. In the current study, a physical model to assess the effect different sizes and locations of a collar around a single cylindrical pier, on clear-water local scour. A three dimensional CFD analysis using ANSYS-FLUENT is conducted to study the effect of the collar on the flow field structure. Based on the experimental results it was concluded that the maximum reduction in non-protected pier local scour depth achieved when the collar located below the bed by 50% of the pier diameter. Increasing the collar diameter at this location will increase the reduction in scour depth. A collar diameter equals four times the pier diameter led to a 53% reduction in the scour depth. 3D CFD simulation using ANSYS-FLUENT commercial package to describe the flow structure in the equilibrium scour hole for both the Unprotected and protected piers. The 4D collar at 0.5D below the original bed level significantly reduced the downward vertical velocity by 20% and reduced the cross-sectional area subjected to the maximum downward velocity.

KEYWORDS: Pier, collar, local scour, down-flow, horseshoe vortex, FLUENT numerical model.

INTRODUCTION

60% of all U.S. bridges failure induced by scouring and soil migration problems[1]. The existence of an obstructive object such as a bridge pier in a flow field leads to the generation of three-dimensional accelerating turbulent flow, and flow vortices which entrain bed sediments in the vicinity of the pier [2]. Figure 1 illustrates the generated vortices in the vicinity of a cylindrical bridge pier located in a stream. This change in the flow field results in the local scours phenomenon around the pier. The horseshoe vortex is a complex vortex system propagates downstream along the pier sides due to the interaction between the downward flow with the coming flow [3]. The horseshoe vortex role in the scour process in the transportation for eroded material outside the scour hole, as the scour hole increases the vortex strength decreases and consequently its ability to transport eroded material. The horseshoe vortex is not the cause of scouring it's a result from the vertical flow generated scour hole [4]. The two vertical vortices located at the downstream side of the pier are defined as wake vortices [5], generated due to flow separation at pier sides. The wake vortices alternate form pier side to the other and its strength decreases along the downstream. Wake and horseshoe vortices remove the eroded soil downstream the scour hole, and when their strength has reduced the deposition of the eroded soil occurs [6].

The foundation level of bridge piers should consider the maximum expected scour depth whenever economical, on the other hand, for very deep scour depths piles (deep foundations) can provide a more economical solution, in addition, to scour countermeasures. The scour countermeasures provided by researchers can be divided into two categories, the first by bed material armoring, and the second by flow altering measures [7]. The collar is usually attached to the pier at a near bed level, belongs to flow altering scour countermeasures since it divides the vertical flow into two parts. The first part above the collar which is obstructed by the collar itself and the second one is below the collar with low scour potential [8]. The reduction of the vertical flow strength reduces the generated horseshoe vortex and lower the sediment transport potential.

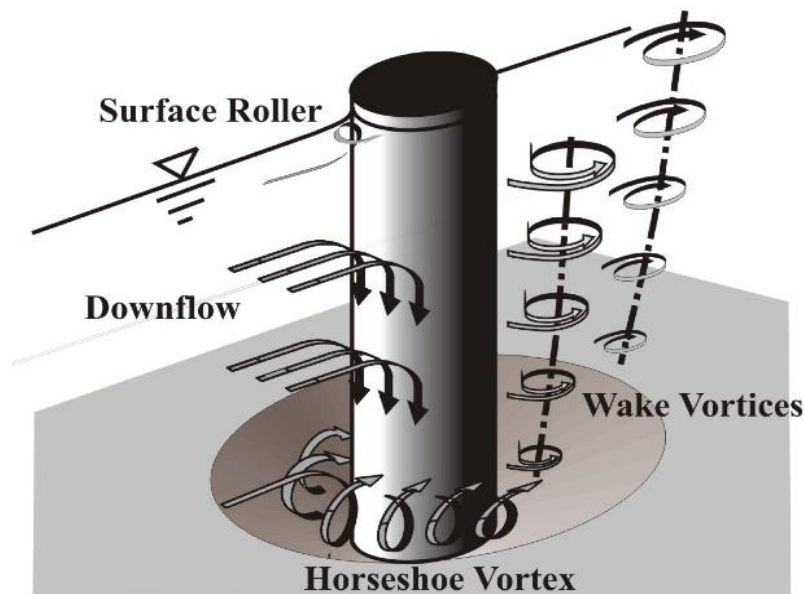


Fig. 1: Generated Vortices around pier [7].

In this study, ANSYS-FLUENT commercial package is utilized to conduct a three dimensional CFD simulation to describe the flow structure in the equilibrium scour hole for both the Unprotected and protected piers

EXPERIMENTAL SETUP AND CONSTRAINTS

The physical model constructed in the Hydraulics Laboratory at the Irrigation and Hydraulics Department, Faculty of Engineering, Cairo University. The cylindrical pier is represented by a 40 mm Plexiglas pipe, and the used collars are 3mm. Plexiglass circular collars with diameters (2.0 D, 3.0 D, and 4.0D) where (D) is the pier diameter, as shown in **Error! Reference source not found.**. The used flume has epoxy coated walls, and fair face concreted bed. The dimensions of the flume are 5.2 m long, 1.0 m wide, and 0.3 m depth. The sediment working section has the full width of the flume, and located at 2.5 m from the flume entrance, with 1.3 m length, and lowered by 20 cm below the flume bed to contain the sedimentary material. The flume is provided by end tailgate to control the flow depth. The flow system is a circulating system, collected at a sum and re-pumped to the flume. The pump is an axial pump with a maximum capacity of 75 liters/sec delivery pipe is provided by a rotating flow meter located at the upstream of a gate valve used in discharge control. The pumped flow turbulence is reduced by using a discharge box of cobbles (5-10 cm. diameter) ending with a 5 mm. steel mesh, as shown in Fig. 3. A point gage with accuracy 0.1 mm is utilized to measure flow depth, a scour hole surveying. The used sand is of mean particle size ($d_{50}=0.5$ mm), uniformly distributed with a geometric standard deviation of 1.3, a specific gravity of 2.65, and an angle of repose 30° . The mechanical sieving and angle of repose test are shown in Fig. 4, and the grain size distribution is shown in Fig. 5.

In order to eliminate the impact of experimental model size on the generated scour hole, the following criteria stated in literature were considered as shown in Table. 1.

Table. 1. Recommended parametric criteria.

Limitation	Used Values
Flume width /Pier Diameter > 8 [9]	25
Pier width (D)/ Mean Grain Size (D_{50}) > 50 [10]	80
Water depth (H_0)/Pier diameter (D) > 3.5 [11]	4.11
Threshold velocity = 0.95 approach velocity [12] and [8]	Same as required

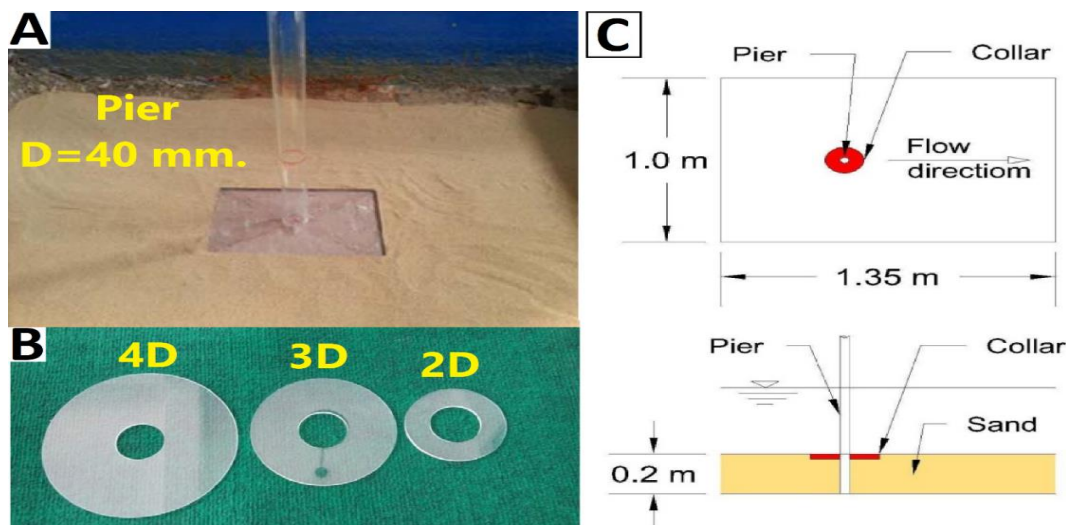


Fig. 2. (A) photo for the pier, (B) photo for the used collars (C) Schematic diagram for the pier and the collar in the working section at $(Z/D)=0$.

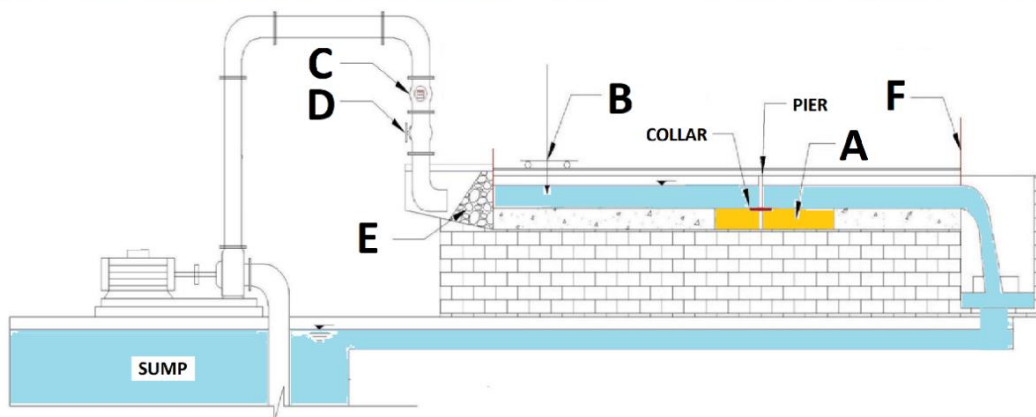


Fig. 3. Schematic diagram for the flume, photograph: (a) working section, (b) point gauge, (c) flow meter, (d) gate valve, (e) cobbles + screen, and (f) Tail gate.

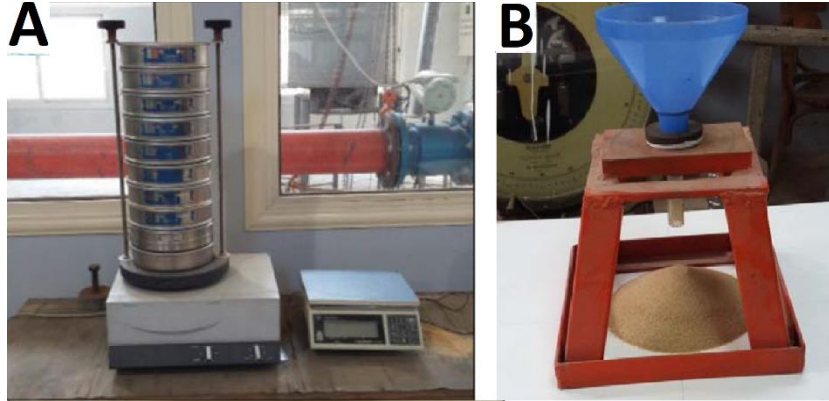


Fig. 4. (A) Mechanical sieving, (B) Angle of repose test.

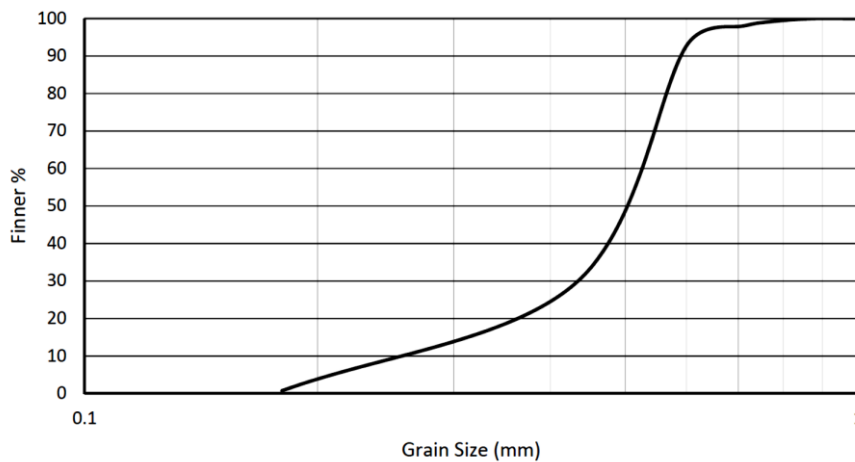


Fig. 5. Grain size distribution.

All experiment has been conducted with discharge 50 liters/sec, and water depth 0.165 m. generated by adjusting the tailgate opening to achieve the velocity of 0.304 m/sec, to ensure the clear water scouring. Initially the local scour around unprotected cylindrical pier was tested to be used as a baseline of comparison with protected ones, and to determine the required time for equilibrium conditions. The maximum scour depth was measured at different times (6, 12, 24, and 36) hours. The equilibrium conditions are achieved when the scour depth variation not more than 5% of the pier diameter during a 24-hour period [12], and [13]. The selected running time (equilibrium time), for the experiments was selected to be 36 hours Figure 6. Shows the variation of the normalized scour depth (d_s/d_{se}) versus (t/t_e), where, (d_s) is maximum achieved scour depth, (d_{se}) is the depth of scour at equilibrium condition, (t) is time, and (t_e) is the equilibrium time (36 hours). it is clear that the scour depth varies rapidly at the early stages of the experiment, then gradually decreases until reaching the equilibrium condition. Figure 6. also shows that about 86% of the scouring depth occurred during the first 20% of the equilibrium time, the maximum scour depth is about $1.96D \approx 2D$ which is in good agreement with [12], [14], [15], and [16]. Figure 7 shows the scour hole for the unprotected pier.

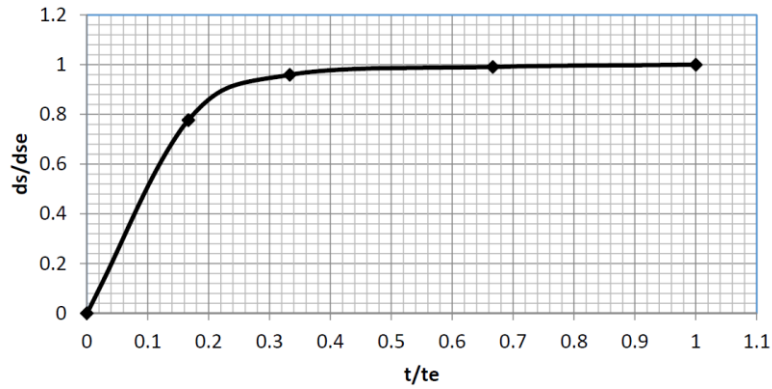


Fig. 6. Development time of local scour around cylindrical pier without Numerical Simulations.

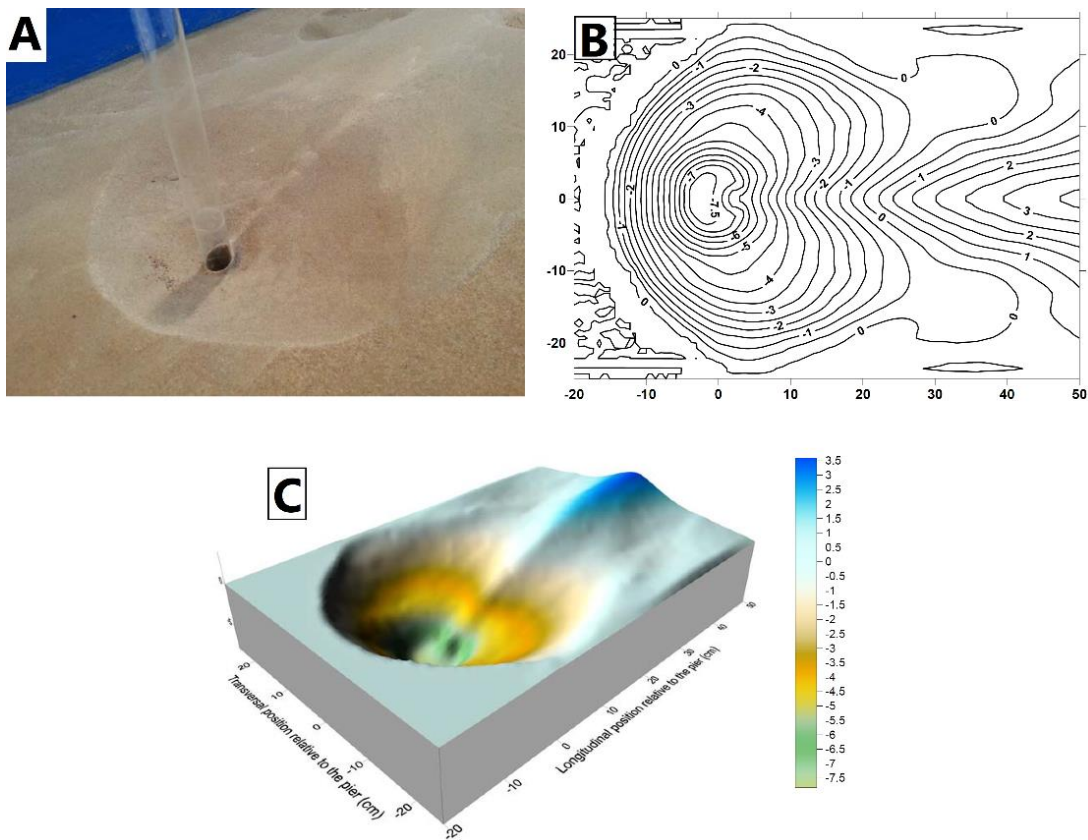


Fig. 7 No collar scour, (A) photo for the scour hole, (B) contour lines for the scour holes in cm, datum = original bed level, (C) 3D surface for the scour hole.

EXPERIMENTAL RESULTS

Eight experiments were conducted for the protected piers with different collar diameters (W), and at different levels (Z) below the original bed level. Figures 7, and 8 illustrates a sample for the collected data for scouring holes at equilibrium conditions. Table 2 summarizes the outcomes of the experiments and the reduction percentage achieved in the scour depth compared to the unprotected piers maximum scour depth.

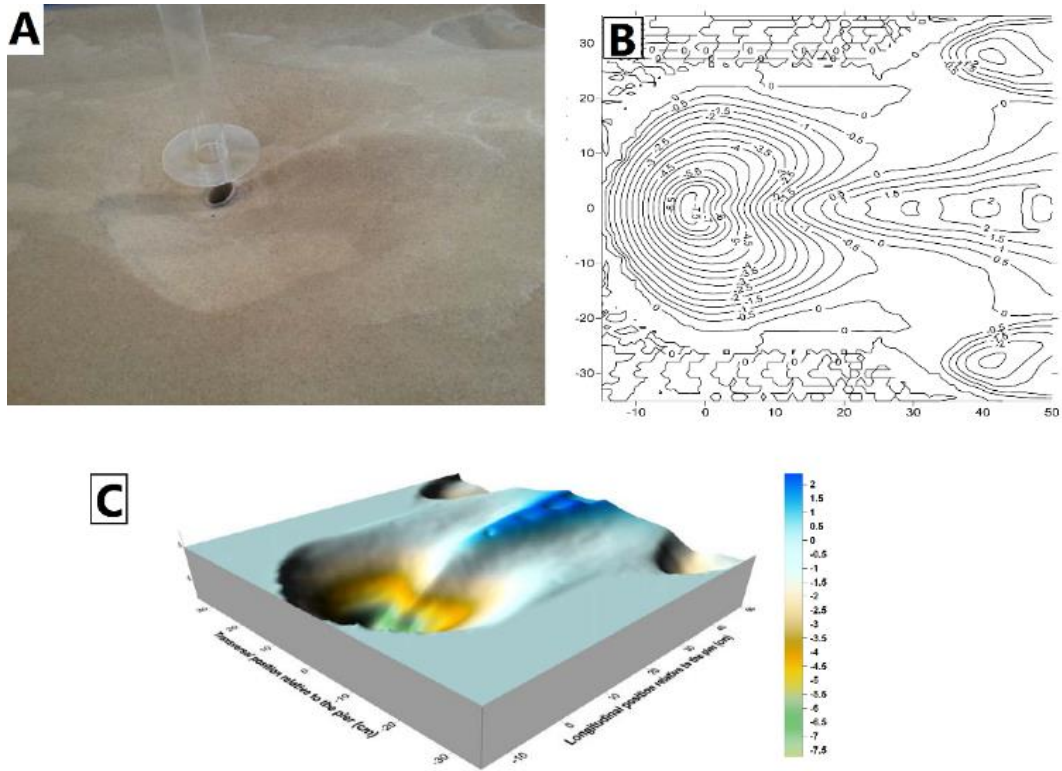


Fig. 8 3D collar at bed level scour hole, (A) photo for the scour hole, (B) contour lines for the scour holes in cm, datum = original bed level, (C) 3D surface for the scour hole.

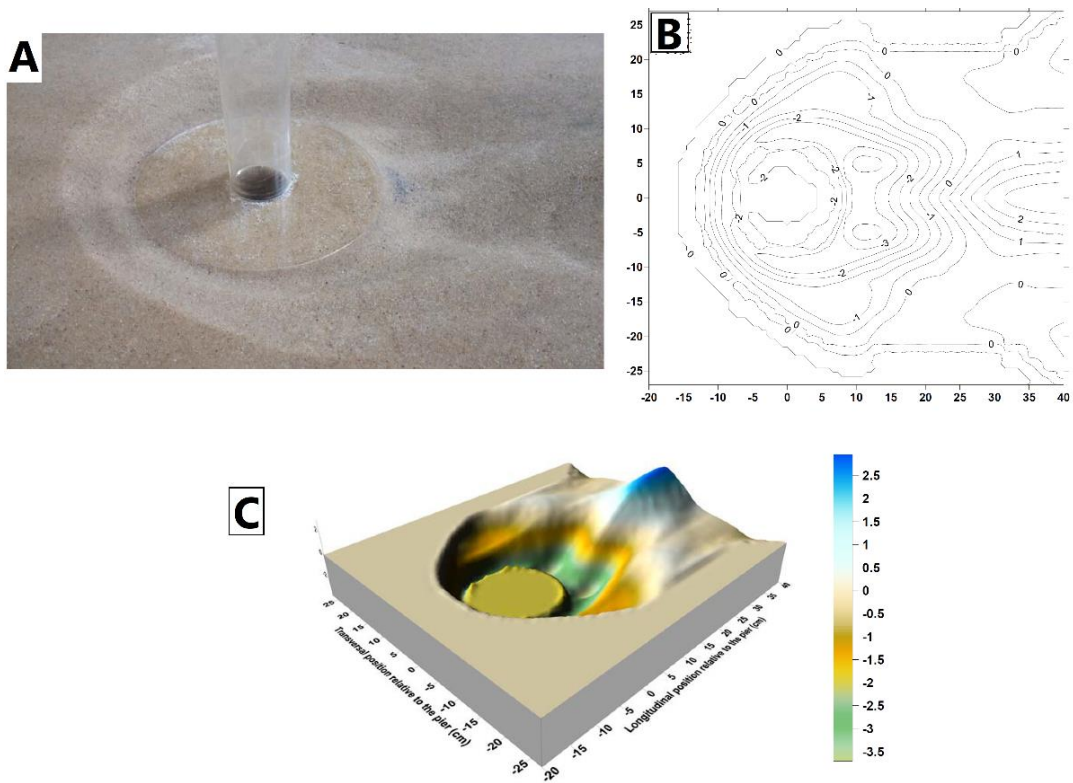


Fig. 9 4-D collar at $-0.5D$ level scour hole, (A) photo for the scour hole, (B) contour lines for the scour holes in cm, datum = original bed level, (C) 3D surface for the scour hole.

Table. 2. Characteristics and results of the experiments.

W/D	Z/D	Scour Depth (cm)	Reduction (%)
..	..	7.85	..
2	-1	5.65	28.03
2	-1.5	6	23.57
3	0	7.75	1.27
3	-0.5	6.75	14.01
3	-1	5.5	29.94
3	-1.5	5.96	24.07
4	-0.5	3.71	52.74
4	-1	4.25	45.86

Figures 10, and 11 illustrate the equilibrium scour hole longitudinal, and transversal profiles for both the collar protected pier and the unprotected pier. It can be concluded that locating the collar at bed level will not reduce the scour hole depth. The maximum reduction in scour reached about 53% by using a 4D collar located at 0.5D below the original bed surface.

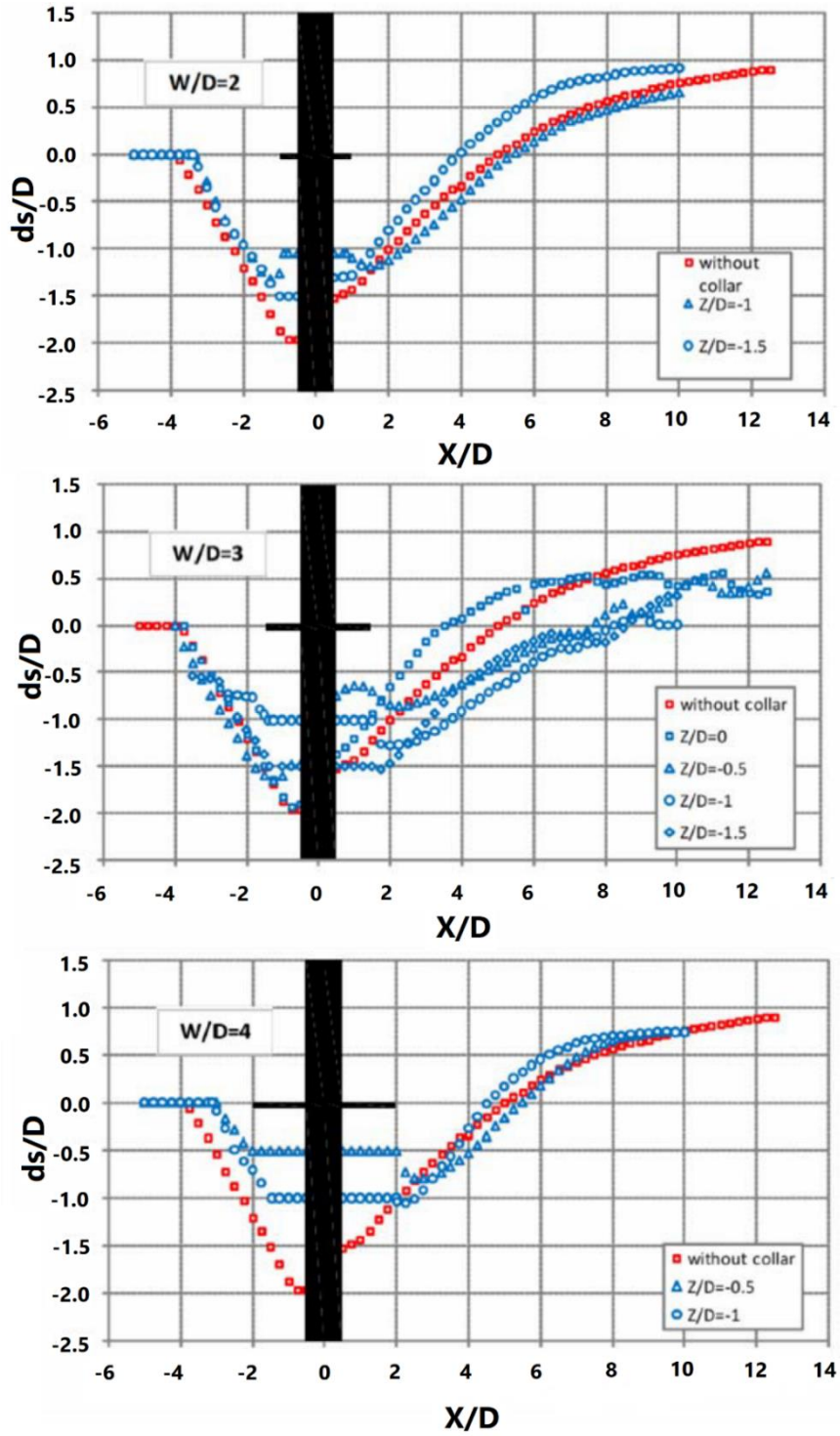


Fig. 10. Comparison between longitudinal profiles at pier center line of the scour hole around a cylindrical pier without a collar, and with a collar at different levels.

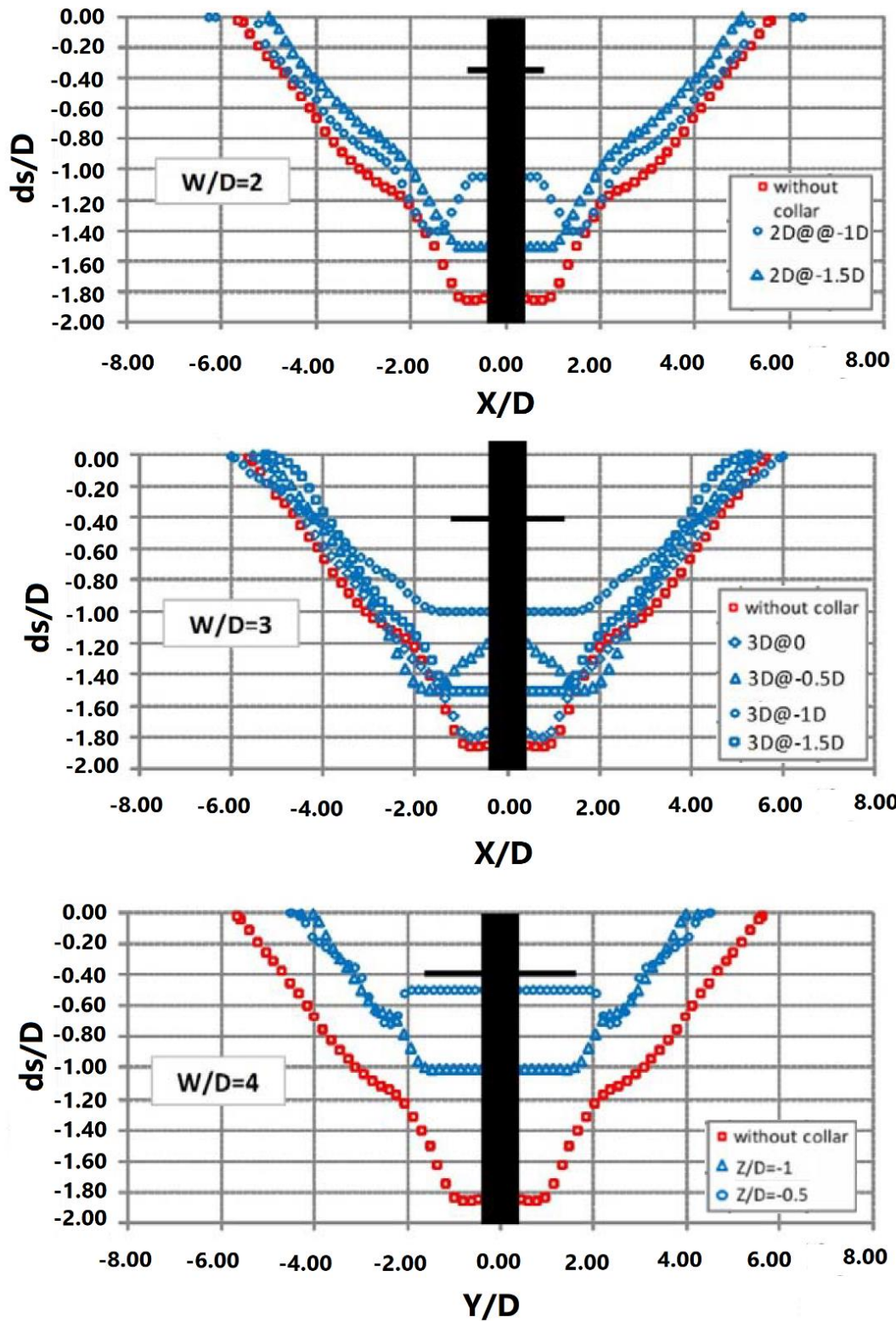


Fig. 11. Comparison between transversal profiles at pier center line of the scour hole around a cylindrical pier without a collar, and with a collar at different levels.

NUMERICAL MODEL

In the present study, a significant reduction in the scour depth by using a 4D collar located at $0.5D$ below the original bed has been experimentally achieved. The collar is classified underflow altering scour countermeasures. In order to assess the impact of the collar on the flow structure a three dimensional numerical CFD model has been conducted using ANSYS-FLUENT commercial software package.

ANSYS-FLUENT is a finite volume based solver, where the Reynolds Averaged Navier Stokes (RANS) governing equations, are integrated over each control volume to construct a linear algebraic discretized equation for each variable. These discretized equations are solving using the implicit method. For modeling, a free surface variation by the ANSYS-FLUENT, and Euler interface capturing technique, known as the volume of fluid (VOF), is used [17].

FLUENT provides multiple choices of turbulence models. In the present study, for all runs, the Renormalized Group RNG $k-\epsilon$ model was used in the simulation as recommended by [18],[19]. There are basically four boundary conditions types defined for the calculation domain: Pressure inlet boundary condition is used to define the fluid total pressure at flow inlet (position, and velocity head), the pressure outlet boundary condition is used to define outlet (water depth), and top boundaries of the domain (atmospheric pressure), symmetry boundary condition is used to define the longitudinal vertical plane intersecting the pier center, and the no-slip wall boundary condition is used to define the bed, flume walls and cylinder pier boundaries of the domain.

The geometry Files is generated using AUTO-CAD 3D for the flume working section and the generated equilibrium scour hole. Figure 12 shows the dimensions of the computational domain, 3D view of the simulated scour hole and the used boundary conditions.

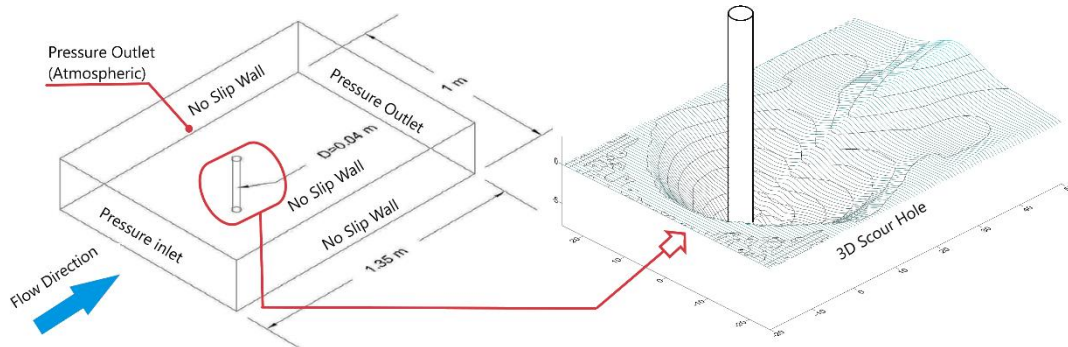


Fig. 12. 3D View for the computational domain and the boundary conditions.

Fine grid is required near the flat and scoured bed as well as the pier surface in order to resolve the flow details near the solid boundaries. Accurate representation of flow near the wall region leads to a successful prediction of the turbulent core of the flow away from the wall. The finer mesh size adjacent to solid boundaries is chosen to satisfy the value of $30 < z^+ < 100$ required to apply the standard wall function by avoiding the calculation in the viscous sublayer. and ensure that the law of the wall is applicable z^+ should be in the range of (Where (z^+) is a dimensionless parameter, (z) distance to the wall with the friction velocity (u^*), and kinematic viscosity (ν) as follow:

$$z^+ = \frac{u^* z}{\nu} \quad (1)$$

According to experiments conditions, the near wall mesh thickness should be in the range of $3 \text{ mm} < z < 9 \text{ mm}$. The size function tool in GAMBIT is utilized to generate a variable size mesh starts from 5 mm up to 20 mm with a 1.05 growth rate.

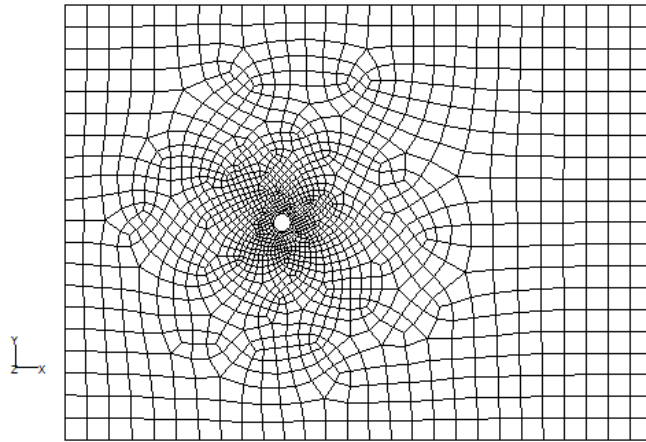


Fig. 13. Plan for the variable size unstructured mesh generated by GAMBIT.

Two simulations were generated for the unprotected pier and the protected pier with collar size $4D$ located at $0.5D$ below the original bed. The coordinate system and the selected sections to view the numerical simulation results are shown in Fig. 14.

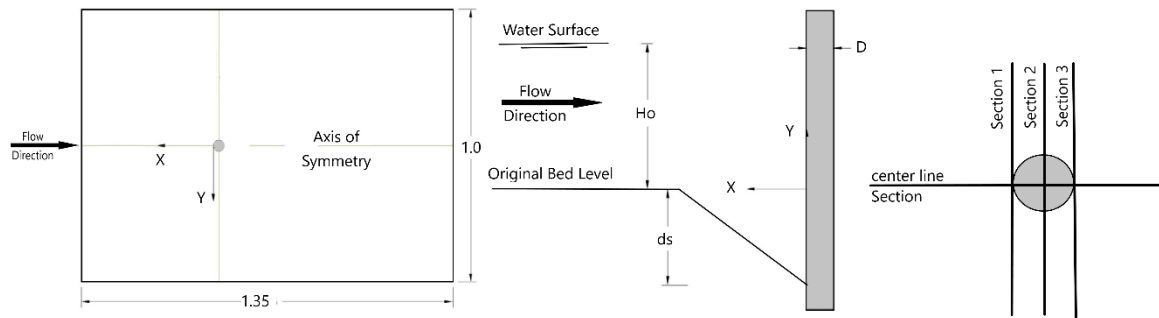


Fig. 14. Coordinate systems and studied sections.

NUMERICAL RESULTS

The contours of the longitudinal velocity component (V_x) along the symmetry plane passing through the pier center for both the unprotected pier and the protected pier with $4D$ collar located at $0.5D$ below the original bed level is given in Fig. 15. No significant impact for the collar on the longitudinal velocity can be noticed. The variation in the longitudinal velocity starts at the beginning of the scour hole and vanished at the mound crest for both cases.

The contours of the variation of vertical velocity component V_z along the symmetry plane passing through the pier center for both the unprotected pier and the protected pier with $4D$ collar located at $0.5D$ below the original bed level is given in

Fig. 16., and the lateral distribution along sections 1,2, and 3 is shown in Fig. 17.

For both cases in the pier upstream side, the vertical velocity is in a downward direction, except a very small part in an upward direction just below the water surface. Two cores of the maximum downward vertical velocity are observed at pier upstream

side the first one at the beginning of the scour hole and the other at the pier face. The maximum downward vertical velocity at the pier nose is about $0.3U_o$, and $0.24U_o$ for the unprotected, and the protected pier respectively which represents about 20% reduction. The cross section area affected by the maximum downward velocity at the pier nose for the protected pier is smaller than the affected area of the unprotected pier.

For the transversal sections 2 and 3, a significant reduction in the area affected by the downward velocity is achieved.

For both cases along the symmetrical section downstream the pier, upward velocity dominates the regions, and becomes negligible after the mound crest. A traces of the downward velocity can be noticed in the transversal section along the pier sides with a maximum value of about $0.1U_o$.

It can be concluded the existence of the collar reduced the vertical velocity by about 20%, and reduced the cross-sectional areas subjected to the maximum downward vertical velocity.

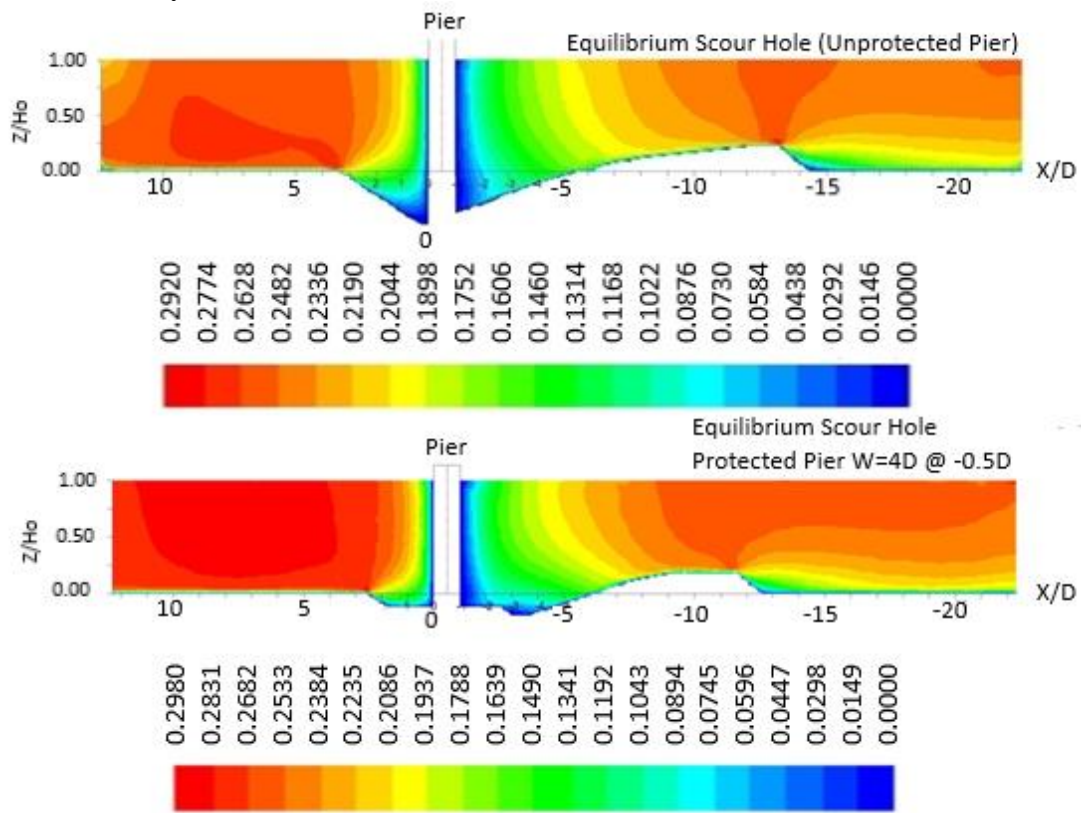


Fig. 15. Longitudinal velocity contour lines at the symmetry plane for both protected and unprotected pier (m/sec).

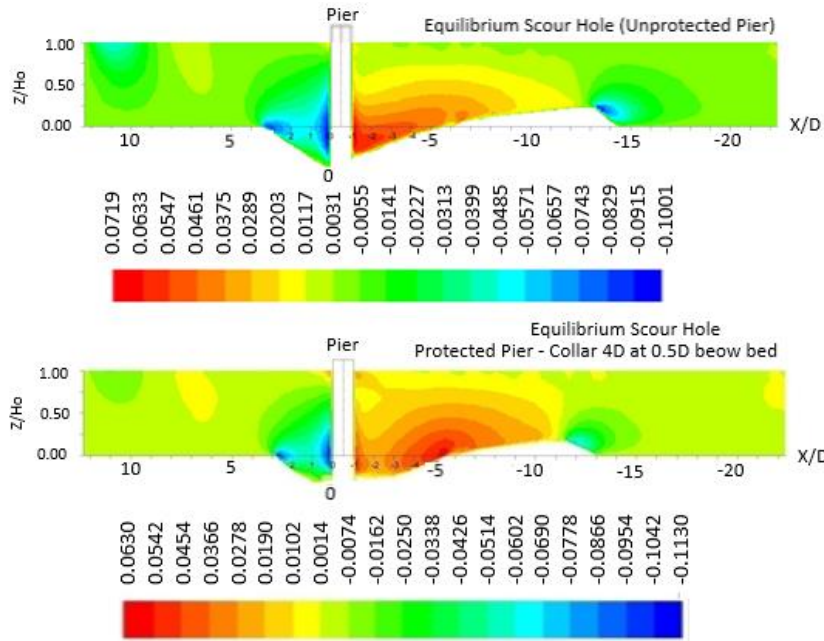


Fig. 16. Vertical velocity contour lines at the symmetry plane for both protected and unprotected pier (m/sec).

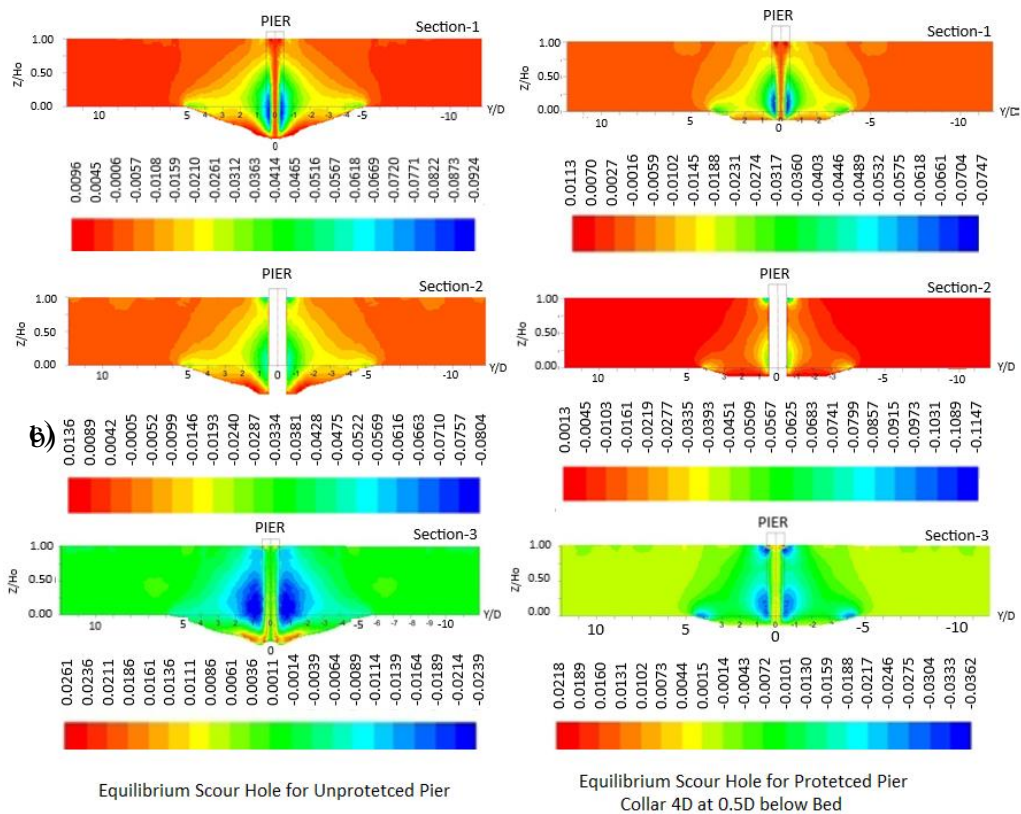


Fig. 17. Variation of the vertical velocity along transversal sections 1,2, and 3 for both protected and unprotected pier (m/sec).

CONCLUSION

Nine experiments have been conducted in the hydraulics laboratory at the Faculty of Engineering, Cairo University, to assess the clear water local scour for both unprotected single cylindrical pier, and collar protected ones. Three collar diameters (2D, 3D, 4D) were examined at different elevations (0, 0.5D, 1.0D, 1.5D) below the original bed level, where (D) is the pier diameter. The maximum reduction in scour depth reached about 53% by using a 4D collar located at 0.5D below the original bed surface.

3D CFD simulation using ANSYS-FLUENT commercial package to describe the flow structure in the equilibrium scour hole for both the unprotected and protected piers. The 4D collar at 0.5D below the original bed level significantly reduced the downward vertical velocity by 20% and reduced the cross-sectional area subjected to the maximum downward velocity.

REFERENCES

- Peter, F. L., and Everett, V. R., "ASCE Compendium of Stream Stability and Bridge Scour papers", Hydraulic Engineering, Vol. 127, No. 7, pp. 531–533, 2001.
- Lauchlan, C. S., and Melville, B. W., "Riprap Protection at Bridge Piers", Hydraulic Engineering, Vol. 127, No. 5, pp. 412–418, 2001.
- Breusers, H. N. C., Nicollet, G., and Shen, H. W., "Local Scour Around Cylindrical Piers," Hydraulic Research, Vol. 15, No. 3, pp. 211–252, 1977.
- Breusers, H. N. C., and Raudkivi, A., "Hydraulic Structures Design Manual-Scouring", International Association for Hydro-Environment Engineering and Research (IAHR), 1991.
- Dargahi, B., "Controlling Mechanism of Local Scouring", Hydraulic Engineering, Vol. 116, No. 10, pp. 1197–1214, 1990.
- Arneson, L. A., Zevenbergen, L. W., and Clopper, P. E., "Evaluating Scour at Bridges", U.S. Department of Transportation, Federal Highway Administration, Hydraulic Engineering Circular No. 18, 2012.
- Melville, B. W., "The physics of local scour at bridge piers", Proceeding of 4th International Conference on Scour and Erosion, No. 1, pp. 28–40, 2008.
- Melville, B. W., and Coleman, S. E., "Bridge Scour", Water Resources Publications, LLC, Colorado, U.S.A., 2000.
- Shen, H. W., Schneider, V. R., and Karaki, S., "Local Scour Around Bridge Piers," Hydraulic Division, Vol. 95, No. 5, pp. 1919–1940, 1969.
- Ettema, R., "Influence of Bed Material Gradation on Local Scour," Report No. 124, School of Engineering, Auckland University, New Zealand, 1976.
- Chiew, Y. M. , and Melville, B. W., "Local scour around bridge piers", Hydraulic research, Vol. 25, No. 1, pp. 15–26, 1987.
- Melville, B. W., and Chiew, Y.-M., "Time Scale for Local Scour at Bridge Piers" Hydraulic Engineering, Vol. 125, No. 1, pp. 59–65, 1999.

- Sheppard, D. M., Odeh, M., and Glasser, T., “Large Scale Clear-Water Local Pier Scour Experiments”, *Hydraulic Engineering*, Vol. 130, No. 10, pp. 957–963, 2004.
- Mashahir, M. B., Zarrati, A. R., Rezaei, M. J., and Zokaei, M., “Effect of Collars and Bars in Reducing the Local Scour Around Cylindrical Bridge Piers”, *International Journal of Engineering*, Vol. 22, No. 4, pp. 333–342, 2009.
- Raudkivi, B. A. J. and Ettema, R., “Clearwater scour at cylindrical piers”, *Hydraulic Engineering*, Vol. 109, No. 3, pp. 338–350, 1983.
- Melville, B. W., and Sutherland, A. J., “Design Method for Local Scour at Bridge Piers”, *Hydraulic Engineering*, Vol. 114, No. 10, pp. 1210–1226, 1988.
- Richardson, J. E., and Panchang, V. G., “Three Dimensional Simulation of Scour Inducing Flow at Bridge Piers”, *Hydraulic Engineering*, Vol. 124, No. 5, pp. 530–540, 1998.
- Salaheldin, T. M., Imran, J., and Chaudhry, M. H., “Numerical Modeling of Three-Dimensional Flow Field Around Circular Piers”, *Hydraulic Engineering*, Vol. 130, No. 2, pp. 91–100, 2004.
- Ahmed, H. S., Ahmed, M. H., and Ahmed, W. A., “3D Numerical Investigation of Flow Field and Horseshoe Vortex Generation Around a Bridge Pier During Scouring Process”, Ph.D. Thesis, Faculty of Engineering, Cairo University, Giza, Egypt, 2013.

ABBREVIATIONS

- Q = discharge.
 H_o = flow depth.
 U_o = mean velocity.
 U_c = critical shear velocity.
D = pier diameter.
W = collar diameter.
Z = collar elevation.
 d_{se} = equilibrium scour depth.
 M_h = height of mound.
 V_s = scour hole volume.
 V_c = scour hole volume with collar.
 V_w = scour hole volume without a collar.
 R_p = percentage of scour depth reduction.